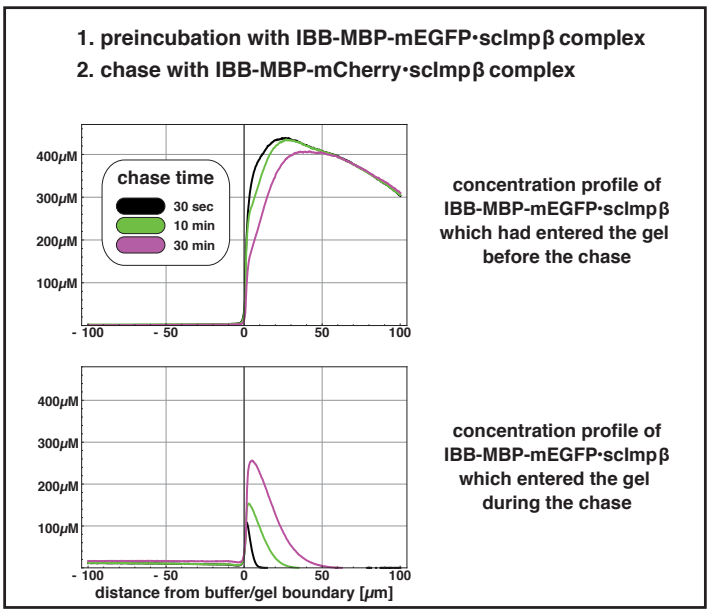

Supplementary Figure S1: Preincubation of the FG/FxFG hydrogel with excess of IBB-MBP-mEGFP• scImpβ complex does not block the gel for subsequent facilitated influx.

A saturated FG/FxFG hydrogel was preincubated for 6.5 hours with 13 μM IBB-MBP-mEGFP•scImpβ complex. The green NTR•cargo complex in the buffer was then exchanged for an analogous red complex (13 μM IBB-MBP-mCherry•scImpβ), and the distribution of both complexes was measured by confocal laser scanning microscopy at the indicated intervals.

Note that the newly added NTR•cargo complex could efficiently enter the gel, even though the gel had been pre-loaded with a concentration of the NTR•cargo complex that essentially precluded passive entry of GFP-sized objects (see Figure 4).

Frey and Görlich, 2009

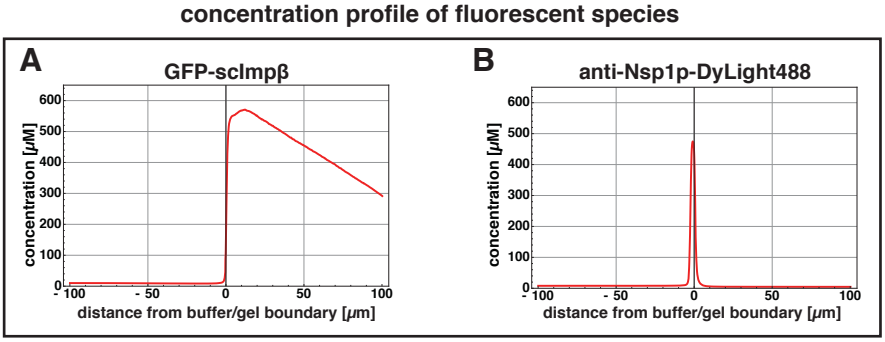

Supplementary Figure S2: The interaction of an FG/FxFG repeat hydrogel with scImpβ is fundamentally different from its interaction with an anti-FG repeat antibody.

A saturated FG hydrogel was prepared from the FG/FxFG repeat domain of Nsp1p and incubated for 3h with either 10 μM GFP-scImpβ (**A**) or 10 μM of a DyLight488-labelled, affinity-purified polyclonal antibody directed against the repeats (**B**).

Graphs show concentration profiles of the fluorescent species across the buffer-gel boundary. While GFP-scImpβ migrated deep into the gel, the anti-FG repeat antibody remained stuck at the surface of the gel, where it reached a similar concentration of 480 μM ($\approx$ 70 mg/ml) as the GFP-scImpβ fusion (570 μM; $\approx$ 70 mg/ml). This observation suggests that a mere binding of macromolecules to an FG hydrogel is not sufficient for mediating facillitated transport.

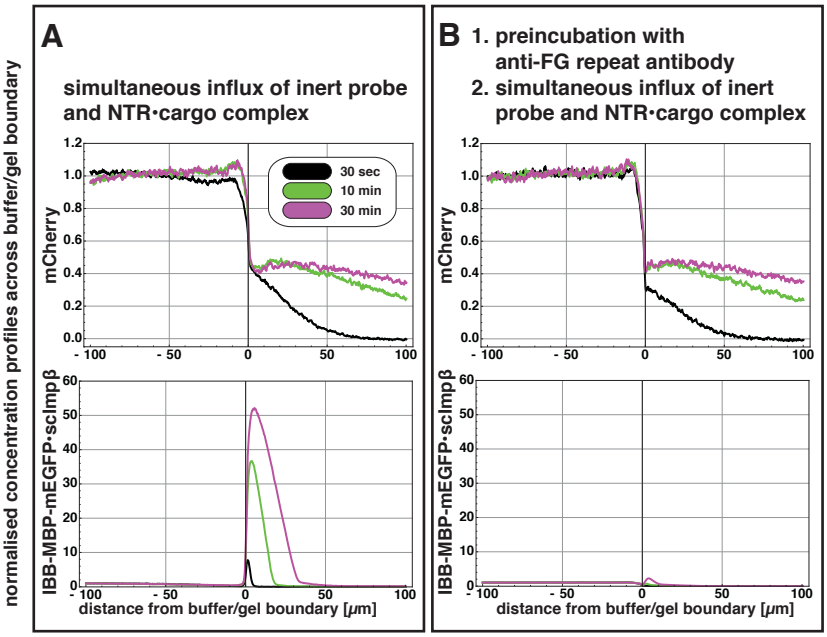

Supplementary Figure S3: Pre-Incubation with an anti-FG repeat antibody drastically reduces the selectivity of an FG/FxFG repeat hydrogel .

An Nsp1p FG/FxFG hydrogel was either left untreated (A) or pre-incubated for 3 h with 10 μM of an affinity-purified polyclonal antibody directed against the FG/FxFG repeats of Nsp1p (B). The antibody was the same as in Supplementary Figure S2, but it was used in an unlabelled form. Then, similar to the experiment shown in Fig. 4, mCherry and the IBB-MBP-mEGFP•scImpβ complex were allowed to simultaneously enter each of the gels.

In contrast to the results obtained after pre-incubation with scImpβ (Fig. 3) or with the IBB-MBP-mEGFP•scImpβ complex (Fig. 4), the antibody treatment had no significant effect on passive influx, but instead dramatically blocked facilitated gel entry (at least a 100-fold inhibition).

The selectivity of the barrier can be expressed as the ratio of facilitated and passive influx. While this ratio is increased upon pre-incubation with scImpβ or scImpβ•cargo complexes (Fig. 3), the antibody pre-treatment decreased the selectivity of an FG/FxFG-hydrogel by at least two orders of magnitude. Thus, the interaction of scImpβ with the gel is fundamentally different from the antibody•hydrogel interaction.

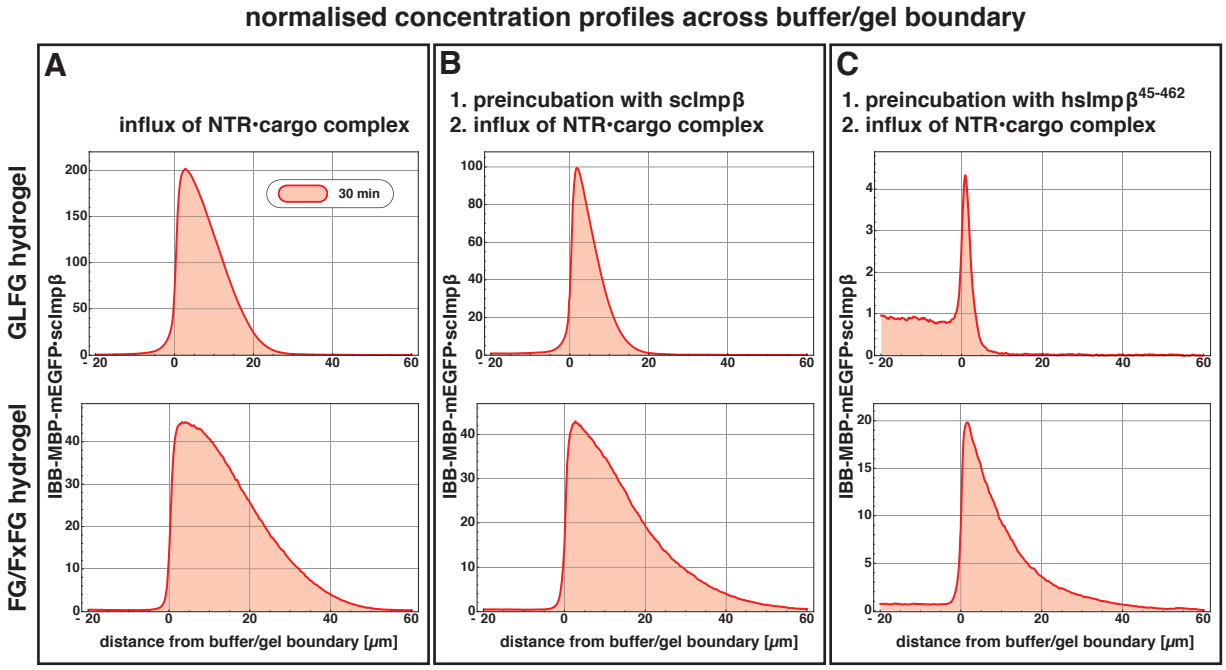

Supplementary Figure S4: GFLG and FG/FxFG hydrogels differ in their response to preincubation with scImpβ or the hsImpβ$^{45-462}$ fragment.

Saturated GLFG (upper panels) or FG/FxFG hydrogels (bottom panels) were prepared and either used without preincubation (**A**) or after 180 minutes of preincubation with 10 μM scImpβ (**B**) or 10 μM of the dominant negative hsImpβ$^{45-462}$ fragment (**C**). Concentration profiles of IBB-MBP-mEGFP•scImpβ complex after 30 minutes influx into these gels are shown.

The figure partially recapitulates data shown in Figure 5. However, for better comparison of intra-gel movement, each profile was scaled to its maximum concentration. Note that in the GLFG hydrogel (upper panels) the dominant-negative hsImpβ$^{45-462}$ mutant (**C**) did not only drastically reduce the enrichment of the NTR•cargo complex at the buffer/gel boundary, but also slowed down diffusion within the hydrogel. In comparison, full length scImpβ (**B**) had less pronounced effects on both parameters. The FG/FxFG hydrogel (lower panels) was far more resistant towards pre-incubation with either scImpβ (B) or the hsImpβ$^{45-462}$ fragment (C).

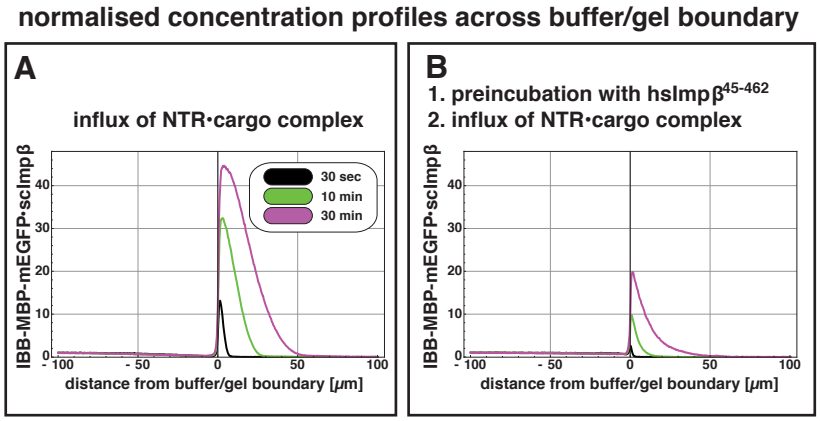

Supplementary Figure S5: The dominant-negative hsImp$\beta^{45\text{-}462}$ fragment only has a weak effect on facilitated influx into an FG/FxFG hydrogel

The figure recapitulates data shown in Figure S4, however, several time points are shown and profiles are drawn at identical scale.

A saturated FG/FxFG hydrogel was prepared as in Figure 3 and either used without preincubation (**A**) or after preincubation for 180 minutes with 10 μM of the hsImp$\beta^{45\text{-}462}$ fragment (**B**). Concentration profiles of IBB-MBP-mEGFP•scImpβ complex at indicated time points are shown.

Note that the dominant-negative hsImp$\beta^{45\text{-}462}$ mutant clearly inhibited the facilitated influx, however, the effect was still weak compared to its drastic effect on the GLFG gel (see Figure 5).

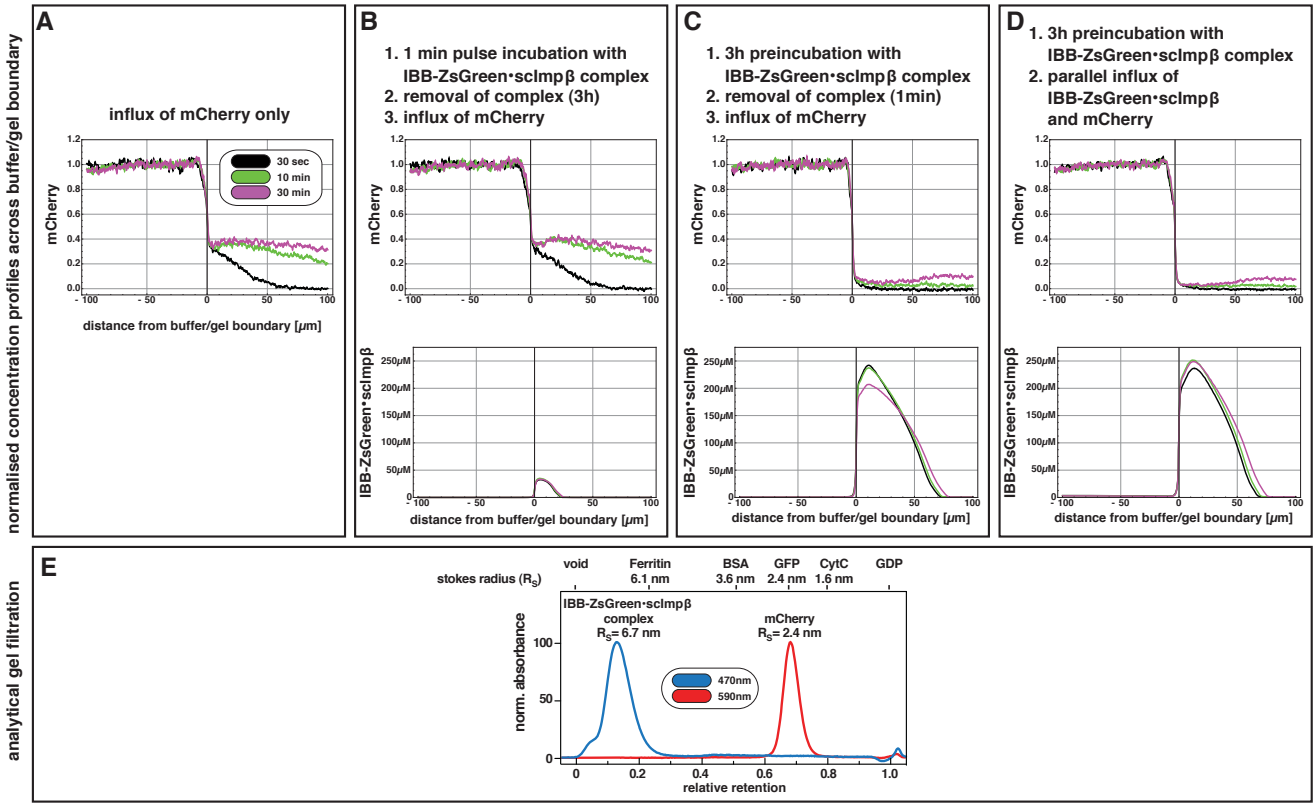

Supplementary Figure S6. The FG/FxFG hydrogel retains its barrier function towards small proteins even when challenged with a large NTR•cargo complex

A-D, Influx of mCherry (29 kD, R_S= 2.4nm) into an FG/FxFG hydrogel was analysed without pre-incubation (A), after 1 min pre-incubation with 2.5 μM of the tetrameric IBB-ZsGreen•scImpβ complex (500 kD, R_S= 6.7nm) followed by a 3 hours wash-out period (B), and after 3 hours continuous pre-incubation with the same NTR•cargo complex in the buffer (C and D). In contrast to C, the NTR•cargo complex was present in D also during influx of mCherry.

Note that none of the pre-incubation schemes led to an increased influx of mCherry into the FG/FxFG hydrogel. Even on the contrary: Prolonged pre-incubation with NTR•cargo complex even tightened the hydrogel towards influx of inert cargo. Thus, perforations transiently formed by ingressing NTR•cargo complexes are not accessible to an inert permeation probe and must therefore rapidly and efficiently reseal behind a translocating species.

E, Analytical gel filtration of mCherry and the IBB-ZsGreen•scImpβ complex used for the experiments in A-D.

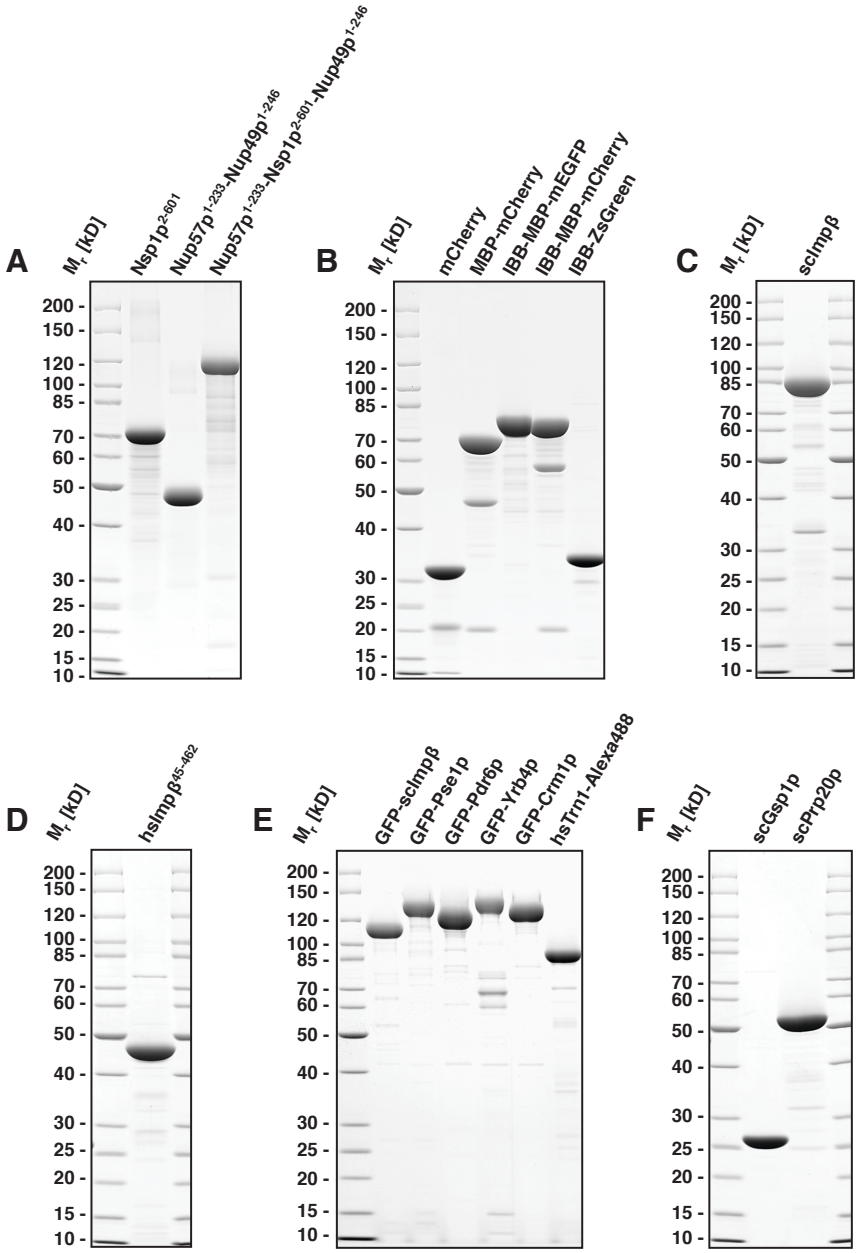

Supplementary Figure S7 : Quality of purified recombinant proteins used in this study.

2.5 μg (A-D, F) or 1 μg (E) of indicated purified recombinant proteins were run on 10% or 7-14% SDS-PAGE gels and stained with Coomassie Brilliant Blue G250.

A: Proteins used for preparation of FG hydrogels

B: Fluorescent proteins used for gel influx and efflux experiments (Figures 2-9, S1 and S3-S6)

C: scImpβ used for gel influx experiments (Figures 2-5, 6, 7, S1 and S3-S6) in conjunction with IBB fusion proteins shown in B.

D: hsImpβ$^{45\text{-}462}$ mutant used for influx inhibition experiments (Figures 5, S4, S5)

E: Fluorescent transport receptors used for gel influx and efflux experiments (Figures 6, 9)

F: Gsp1p and Prp20p used for efflux experiments (Figure 9)